ICOT Technical Report: TR-368

TR-368

Control of an Active Suspension System for a Wheeled Vehicle

by
E. Horiuchi, S. Usui, K. Tani & N. Shirai

April, 1988

ICOT
Mita Kokusai Bldg. 21F
4-28 Mita 1-Chome
Minato-ku Tokyo 108 Japan
(03) 456-3191~5
Telex ICOT J32964

Institute for New Generation Computer Technology

Control of an Active Suspension System for a Wheeled Vehicle

E. HORIUCHI, S. USUI, K. TANI, N. SHIRAI

Namiki 1-2, Tsukuba-city, Ibaraki 305 Japan
Mechanics Division,
Robotics Department
Mechanical Engineering Laboratory

Abstract
An active suspension system with an actuator in parallel with a spring and a shock absorber is designed for a wheeled vehicle. The passive elements in the mechanism reduce high frequency vibration. A possible implementation with a DC torque motor and a pseudo-straight line mechanism is illustrated. A simple analysis of the kinematics of a wheeled vehicle with an active suspension is also discussed. A control method based on sliding mode control is developed for a two-wheeled two degree of freedom model of the vehicle. Simulation results show that, in the sense of root-mean-square vibration reduction, active suspension is superior to passive suspension and that proposed approaches are effective when applied to a nonlinear system.

1 Introduction

Recently, the use of wheeled vehicles in inaccessible and dangerous environments is increasing. The transport of wood or planting work in forests, rescue activities in the area hit by a disaster, and maintenance and inspection work in nuclear plants are examples of possible practical applications of wheeled vehicles. A wheeled vehicle which aims at traveling over irregular terrains needs a specific suspension system in place of conventional passive devices, a spring or a shock absorber, employed as suspensions for ordinary vehicles. The suspension system required for such a vehicle must be provided with actuators to have the accommodation to terrains and realize the suspension properties suited for the vehicle function.

Energy consumption by active suspension systems is an important problem because practicable wheeled vehicles should be self-contained. Semi-active suspensions [1],[2] are alternatives for this problem. They use an active damper in parallel with a passive spring. In this paper, a concept of an active suspension system (AS) composed of passive elements and an actuator as well as a suspension controller design is presented. So far, several

optimum control strategies based on linear models have been studied: optimum output feedback control [3] and preview control [4] (a control scheme in which an input is sensed before it reaches the controlled plant). This paper employs a control strategy based on sliding mode control [5] for AS.

2 Active suspension system

2.1 Concept of an active suspension system (AS)

The concept of AS is shown in Fig. 1. This system has an actuator generating a force f(t) in the vertical direction, a spring with stiffness K, and a shock absorber with damping ratio C in parallel between the vehicle body with mass M and the wheel axle. An unknown terrain elevation r(t) at the wheel is transmitted to the body through the suspension mechanism and causes the body displacement x(t) in the vertical direction. Both x(t) and r(t) refer to some absolute frame. Only the vibration in the vertical direction is considered in the rest of this paper.

2.2 Effect of passive elements

The actuator in AS only has to control the low frequency body vibration because the spring sustains the static load and the choice of spring stiffness and damping ratio to the given body mass determines the upper bound of the frequency of the vibration to be actively controlled. These passive elements highly reduce the high frequency vibration. To make the effect of them clear, the dynamics of the system shown in Fig.1 is investigated.

$$M\ddot{x}(t) + C\{\dot{x}(t) - \dot{r}(t)\} + K\{x(t) - r(t)\} = f(t) \quad \ldots\ldots(1)$$

From (1) with f(t) = 0, a transfer function G(s) with input r(t) and output x(t) is obtained.

$$G(s) = \frac{Cs + K}{Ms^2 + Cs + K} \quad \ldots\ldots\ldots\ldots\ldots\ldots\ldots\ldots\ldots\ldots(2)$$

The gain diagram of G(s) is shown in Fig. 2. The values of C and K are shown in Table 1, and M = 25 kg. A peak observed at about 2 Hz indicates that the upper bound of the frequency of the vibration to be actively controlled is 2 Hz or so.

2.3 An implementation of the active suspension system

An implementation of AS utilizing the Chebyshev's four-bar link to transform the actuator rotational motion into the pseudo-straight line motion at the wheel axle is shown in Fig. 3. Figure 5 shows the pseudo-straight line motion generated by this

mechanism. The actuator torque is also transformed into the force applying at the wheel axle by way of this structure although the force-torque relationship is dependent on the actuator angle. The force at the axle generated by 1 Nm actuator torque is shown in Fig. 6. A DC torque motor is employed as the actuator of AS since precise open loop torque control is possible because of its small friction, although active suspensions often use hydraulic or pneumatic actuators [6],[7].

3 A two-wheeled two degree of freedom model

3.1 Formulation

A two-wheeled two degree of freedom model of the wheeled vehicle is derived on assumptions that (a) the tires are rigid and (b) the wheels keep contact with the ground. Since the upper bound frequency of the vibration to be actively controlled decreases with decreasing K if C and M are fixed, spring stiffness is desired to be small in spite of the drawback of the large body sink by the gravity. The tires are much more rigid than the spring in AS. The locomotion speed of the vehicle in the scope of this paper is rather slow, so that the vehicle presumedly will not spring free from the ground.

The model shown in Fig. 4 has two degrees of freedom: the body height and the body tilt. If the wheels correspond to the front and rear wheels, $\theta(t)$ is the pitch angle; and if they represent the right and left wheels, $\theta(t)$ is the roll angle. The height of the center of mass of the body, $x_G(t)$, refers to some absolute frame. Subscripts, F and R, indicate that the variable is related to either the F-wheel or the R-wheel. And M, I, and 2L mean the body mass, the moment of inertia of the body, and the body length (wheelbase or tread), respectively. The body length is presumed to be independent of the body tilt and unchanged.

$$y_i(t) = x_i(t) - r_i(t) \ ; \ i = F, R \quad \text{.....(3)}$$

where $y_i(t)$ is the distance between the body and the ground. Formulation should be done in terms of $y_i(t)$ since precise measurement of $x(t)$ and $r(t)$ is difficult. Dynamic equations based on $x(t)$ and $r(t)$ are rewritten by measurable variables. Suppose that the distances between the body and the ground at the suspension positions are available, $y_G(t)$ defined in (4) is introduced as a variable which represents the body height.

$$y_G(t) = \{y_F(t) + y_R(t)\}/2 \quad \text{.....(4)}$$

Let the equilibrium position of the vehicle body the origin, and the dynamic equations concerning the body height and the body tilt based on measurable variables are obtained as follows.

$$M\ddot{y}_G(t) = f_Y(t) - 2C\dot{y}_G(t) - 2Ky_G(t) + d_Y(t) \quad \cdots\cdots\cdots(5)$$

$$I\ddot{\theta}(t) = L\cos\theta(t)\{f_\theta(t) - 2CL\dot{\theta}(t)\cos\theta(t) \quad \cdots\cdots\cdots\cdots(6)$$
$$- 2KL\sin\theta(t)\} + d_\theta(t)$$

where

$$f_Y(t) = f_F(t) + f_R(t),\ f_\theta(t) = f_F(t) - f_R(t)$$

$d_Y(t)$ and $d_\theta(t)$ are disturbance forces caused by unknown terrain elevations to the body height and to the body tilt, respectively. It is assumed that only maximum absolute values of $d_Y(t)$ and $d_\theta(t)$ can be estimated. Note that these equations are decoupled between $y_G(t)$ and $\theta(t)$ by letting $K_F = K_R$ and $C_F = C_R$ and that (6) is nonlinear.

3.2 Kinematics of the wheeled vehicle

The use of $y_G(t)$ in stead of $x_G(t)$ avoids difficult problems in the locomotion over unknown terrains. If $x_G(t)$ is kept unchanged while traveling over a long slope, for example, the limits of the suspension stroke will make it impossible to continue the locomotion. It is necessary to analyze the kinematics of the wheeled vehicle with AS under the condition that $y_G(t)$ and $\theta(t)$ are kept constant.

When $y_G(t)$ and $\theta(t)$ are fixed, the body of the vehicle traveling over a long flat slope follows the slope profile. Consider terrain elevations defined by a sinusoidal function.

$$r_F(t) = \sin 2\pi\omega t,\ r_R(t) = \sin 2\pi\omega(t - B/V)$$

where V is a constant locomotion speed, B is the wheelbase, and ω is the frequency of terrain elevations. If $y_G(t)$ is controlled to be a constant H and $\theta(t)$ is kept zero, then,

$$x_G(t) = \{x_F(t) + x_R(t)\}/2$$
$$= H + \{\sin 2\pi\omega t + \sin 2\pi\omega(t - B/V)\}/2 \quad \cdots\cdots\cdots(7)$$

Consider two cases: (a) $B\omega/V = n$, (b) $B\omega/V = n + 1/2$. In case (a), (7) is reduced to $x_G(t) = H + \sin 2\pi\omega t$. This means that the vehicle body tracks the same trajectory as $r_F(t)$. While in case (b), (7) becomes $x_G(t) = H$ which shows that the height of the vehicle is held fixed with respect to some absolute frame. Considering general cases, the path of $x_G(t)$ becomes a trajectory

with an intermediate amplitude between those two trajectories because the apparent frequency of terrain elevation depends on the locomotion speed and actual terrain profiles cannot be modeled by a simple sinusoidal curve.

4 Sliding mode control

4.1 Purposes of sliding mode control

The nonlinearity in the dynamics of the vehicle with AS should be paid attention to. The fact that, in physical suspension systems, spring stiffness and damping ratio are prone to involve nonlinear and time-varying properties which bring about parameter errors and parameter variations should also be considered. Sliding mode control is one solution to these problems because it is capable of dealing directly with nonlinear systems and needs only estimation values about nonlinearity of the system.
In addition, the vehicle discussed here is planned to be equipped with a vision sensor system which detects obstacle surfaces. Sliding mode control is a simple model following control; the state variables of the system in sliding mode are constrained on defined switching lines. Thus, the correction of sensor data based on the vibration model is possible.

4.2 Design of a sliding mode controller

The design procedure of a controller which regulates $y_G(t)$ and $\theta(t)$ is as follows. First, on the basis of the premise that state variables are available, switching lines for $y_G(t)$ and $\theta(t)$ with negative inclinations are defined in phase plain.

$$s_Y = \dot{y}_G(t) + \alpha_Y y_G(t) = 0 \quad (\alpha_Y > 0) \qquad \text{.....(8)}$$

$$s_\theta = \dot{\theta}(t) + \alpha_\theta \theta(t) = 0 \quad (\alpha_\theta > 0) \qquad \text{.....(9)}$$

Second, the control structure is defined. In this approach, a control strategy which switches between two values according to the sign of s_Y and s_θ is introduced.

$$f_i = \begin{cases} f_i^+ & (s_i > 0) \\ f_i^- & (s_i < 0) \end{cases} \quad ; \; i = Y, \theta \qquad \text{.....(10)}$$

Third, control signals must be determined so that sliding mode exists in the neighborhood of the switching line. The occurrence of sliding mode is assured by global asymptotic stability of an equilibrium point, $s_i = 0$; $i = Y, \theta$, which is proven by the second method of Lyapunov. After the certification of $V(t) = s_i^2$; $i = Y, \theta$ being Lyapunov functions, which is omitted here, next con-

ditions are derived.

$$\dot{s}_i s_i < 0 \ ; \ i = Y, \theta \quad \text{.....(11)}$$

These are sufficient conditions for the occurrence of sliding mode. As for the pitch angle, $\theta(t)$,

$$\dot{s}_\theta = \ddot{\theta} + \alpha_\theta \dot{\theta}$$
$$= L\cos\theta\{f_\theta - 2CL\dot{\theta}\cos\theta - 2KL\sin\theta\}/I + \dot{d}_\theta/I + \alpha_\theta\dot{\theta} \quad (12)$$

In the case that $s_\theta > 0$, from the condition (11), $\dot{s}_\theta < 0$. From (12), the condition to be satisfied by f_θ^+ is obtained.

$$f_\theta^+ < \{2CL\cos\theta - I\alpha_\theta/(L\cos\theta)\}\dot{\theta} + 2KL\sin\theta - d_\theta/(L\cos\theta)$$
$$\text{.....(13)}$$

Each term on the right hand of (13) is minimized with respect to $\theta(t)$. For the simplicity, the parameters, M, I, C, and K, are assumed to be time-invariant and perfectly identified in advance. If they should involve parameter errors or parameter variations, the minimization would have to take their influence into consideration. In this formulation, only the information about maximum and minimum values of parameter errors or parameter variations would be required.

From the premise that maximum absolute values of $d_Y(t)$ and $d_\theta(t)$ are known, minimum values of the second and the third term on the right hand of (13) is obtained with $-\pi/4 \leq \theta \leq \pi/4$.

$$\text{The second term} \geq -\sqrt{2}KL$$

$$\text{The third term} \geq -\sqrt{2}|d_\theta|_{max}/L$$

If $1/\sqrt{2} \leq x \leq 1$ for a function, $f(x) = ax - b/x$ $(a, b > 0)$, then

$$(a - 2b)/\sqrt{2} \leq f(x) \leq a - b$$

Therefore,

$$|f(x)| \leq \beta = \max\{|2CL - I\alpha_\theta/L|, \sqrt{2}|CL - I\alpha_\theta/L|\}$$

$$\text{The first term} \geq -|f(\cos\theta)||\dot{\theta}| \geq -\beta|\dot{\theta}|$$

The desired control law is obtained by combining these terms.

$$f_\theta^+ = -\beta|\dot{\theta}| - \sqrt{2}KL - \sqrt{2}|d_\theta|_{max}/I \quad \text{.....(14)}$$

When $s_\theta < 0$, control law f_θ^- is derived in the same way.

$$f_\theta^- = \beta|\dot{\theta}| + \sqrt{2}KL + \sqrt{2}|d_\theta|_{max}/I \quad \text{.....(15)}$$

As for $y_G(t)$, next control laws are introduced after the similar discussion as above.

$$f_Y^+ = -|2C - M\alpha_Y||\dot{y}_G| - 2K|y_G| - |d_Y|_{max} \quad (s_Y > 0) \quad \text{.....(16)}$$

$$f_Y^- = |2C - M\alpha_Y||\dot{y}_G| + 2K|y_G| + |d_Y|_{max} \quad (s_Y < 0) \quad \text{.....(17)}$$

5 Hybrid control

One demerit of sliding mode control is chattering caused by the delay in physical systems. Suction control [8] which employs continuous control laws to approximate switched control is an approach for rejecting the chattering. A hybrid method which combines sliding mode control with state feedback control, is introduced to overcome this problem.

Consider a system whose dynamics is expressed in the form that

$$M\ddot{x}(t) = u(t) - A\dot{x}(t) - Bx(t) \quad \text{.....(18)}$$

where A, B, and M are positive constants and u(t) is a control signal. For a hybrid controller design, a new parameter, z(t), is introduced.

$$z(t) = \dot{x}(t)/x(t) \quad \text{.....(19)}$$

This parameter indicates the direction in which the point corresponding to the state variables in phase plain converges on the origin of phase plain. When this system is controlled by a state feedback controller,

$$u(t) = -k_1x(t) - k_2\dot{x}(t) \quad \text{.....(20)}$$

with z(t), (18) is reduced to

$$\dot{z}(t) = -z^2(t) - Pz(t) - Q \quad \text{.....(21)}$$

where

$$P = (k_2 + A)/M > 0, \quad Q = (k_1 + B)/M > 0$$

Let z_1 and z_2 $(0 > z_1 > z_2)$ be solutions of the equation

$$z^2 + Pz + Q = 0 \quad \text{.....(22)}$$

If the next condition (23) is satisfied, z_1 and z_2 are negative.

$$P^2 - 4Q > 0 \quad \text{.....(23)}$$

Both z_1 and z_2 can be interpreted as equilibrium points in the space of z of the system described by (21). After a simple analysis, it is proven that the equilibrium point z_1 is locally asymptotically stable for $z > z_2$.

The basic idea on which hybrid control is based is that (a) when the system is subject to disturbances, sliding mode controller draws the state of the system into the neighborhood of z_1 which satisfies $z > z_2$, and (b) once the state enters the domain, the control is switched to state feedback controller which assures that the state remains within the domain until it converges on the origin of phase plain. A division of phase plain is illustrated in Fig. 7. Both $-\alpha_1$ and $-\alpha_2$ are inclinations of boundaries of the domain S^f, where state feedback controller is on. Both S^+ and S^- represent domains in which sliding mode controller is on. The magnitudes of hybrid control parameters, α, α_1, α_2, z_1, and z_2 must follow the next inequality.

$$0 > -\alpha_1 > -\alpha = z_1 > -\alpha_2 > z_2 \quad \text{.....(24)}$$

These parameters provide more intuitive guidelines for controller design than the index performance utilized in optimum control. Let $z_1 = -\alpha$, and feedback gains, k_1 and k_2, are determined from (25) under the condition (23).

$$\alpha^2 - P\alpha + Q = 0 \quad \text{.....(25)}$$

Obtained hybrid control laws are

$$\begin{aligned}
&\text{if } (y_G, \dot{y}_G) \in S_Y^+ \text{ then } f_Y = f_Y^+ \\
&\text{if } (y_G, \dot{y}_G) \in S_Y^- \text{ then } f_Y = f_Y^- \quad \text{.....(26)} \\
&\text{if } (y_G, \dot{y}_G) \in S_Y^f \text{ then } f_Y = -k_{Y1}y_G - k_{Y2}\dot{y}_G \\
&\text{if } (\theta, \dot{\theta}) \in S_\theta^+ \text{ then } f_\theta = f_\theta^+ \\
&\text{if } (\theta, \dot{\theta}) \in S_\theta^- \text{ then } f_\theta = f_\theta^- \quad \text{.....(27)} \\
&\text{if } (\theta, \dot{\theta}) \in S_\theta^f \text{ then } f_\theta = -k_{\theta1}\theta - k_{\theta2}\dot{\theta}
\end{aligned}$$

As for $\theta(t)$, a linearization of (6) is used. In the vicinity of the origin, control signals by the sliding mode controller and the hybrid controller are set zero values.

6. Simulation results and discussion

6.1 Test terrain

The ability of the proposed controllers is verified by the computer simulation of a two-wheeled vehicle with a front and a rear wheel traveling over test terrains. Parameters used in the simulation are listed in Table 1. The test terrain profile, $r_i(t)$, a function of time, is given by an output of a second order system.

$$\ddot{r}_i(t) + a_1\dot{r}_i(t) + a_2 r_i(t) = w(t);\ i = F, R \quad \text{.....(28)}$$

where $w(t)$ denotes a signal to form the test terrain, and both a_1

and a_2 are parameters to specify the smoothness and the amplitude of the test terrain. Test terrains generated by a trapezoid-form signal are shown in Fig. 8.

6.2 Simulation results

The suspension performance is verified among a passive suspension composed of a spring and a shock absorber only and AS with three different control strategies: (1) the optimum regulator, whose diagonal weights of the performance index, Q, are listed in Table 1, (2) the sliding mode controller, and (3) the hybrid controller. The control cycle is 20 msec and control signals are updated when 10 msec is past after the acquisition of new state variables, which takes the computation time and the servo delay into consideration.

Figure 9 shows $y_G(t)$'s and Fig. 10 shows $\theta(t)$'s. Root mean square values of $y_G(t)$'s and $\theta(t)$'s are presented in these figures. It is shown that the body vibration in $y_G(t)$ and $\theta(t)$ is highly reduced by AS and, especially in the case of the body tilt $\theta(t)$ which include nonlinear dynamics, both the sliding mode controller and the hybrid controller achieved better results than those by the optimum regulator. In Fig. 10, the chattering rejection by hybrid control appears in the curve of $\theta(t)$ approaching zero.

Figure 11 depicts the F-wheel actuator forces during the locomotion. Although the sliding mode controller and the hybrid controller generate greater signals than the optimum regulator, the hybrid controller succeeds in smoothing control signals to a certain extent, which leads to the chattering rejection.

7. Conclusion

The main purpose of this paper is the control system design of an active suspension system for a wheeled vehicle for applications in hazardous environments. In the sense of root-mean-square vibration reduction, both sliding mode controller and hybrid controller which generate nonlinear and discontinuous signals achieved comparable suspension performance to optimum regulator based on linear model. In addition, proposed hybrid method which gives intuitive control specifications succeeded in reducing the chattering. Future work will treat the design of a new active suspension system for a four-wheeled vehicle with six degrees of freedom and the extension of the proposed control strategies to

the six-degree-of-freedom model.

References

[1] D.Karnopp, M.J.Crosby, R.A.Harwood: Vibration Control Using Semi-Active Force Generators, ASME Journal of Engineering for Industry, pp.619/626 (1974)
[2] J.Alanoly, S.Sankar: A New Concept in Semi-Active Vibration Isolation, ASME Journal of Mechanisms, Transmissions, and Automations in Design, Vol.109 pp.242/247 (1987)
[3] A.G.Thompson, B.R.Davis, F.J.M.Salzborn: Active Suspensions with Vibration Absorbers and Optimal Output Feedback Control, SAE Technical Paper No.841253 (1984)
[4] E.K.Bender: Optimum Linear Preview Control With Application to Vehicle Suspension, ASME Journal of Basic Engineering pp.213/221 (1968)
[5] V.I.Utkin: Variable Structure Systems with Sliding Modes, IEEE Transactions, Vol.AC-22, No2 pp.212/222 (1977)
[6] D.Cho, J.K.Hendrick: Pneumatic Actuators for Vehicle Active Suspension Applications, ASME Journal of Dynamic Systems, Measurement, and Control, Vol.107 pp.67/72 (1985)
[7] J.Dominy, D.N.Bulman: An Active Suspension for a Formula One Grand Prix Racing Car, ASME Journal of Dynamic Systems, Measurement, and Control, vol.107 pp.73/78 (1985)
[8] J-J.E.Slotine: The Robust Control of Robot Manipulators, The International Journal of Robotics Research, Vol.4 pp.49/64 (1985)

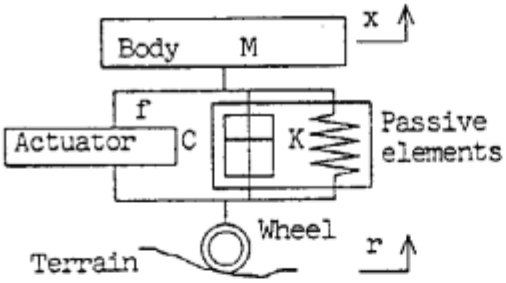

Fig. 1 Concept of AS

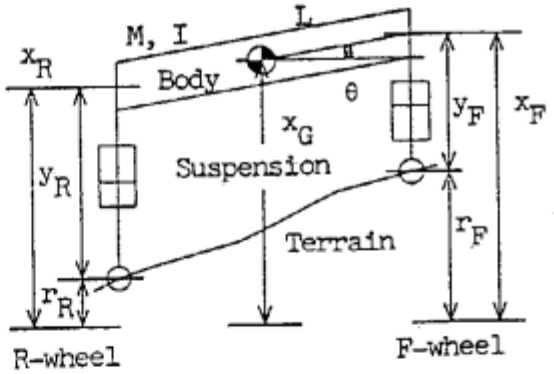

Fig. 4 Two-wheeled two d.o.f. model

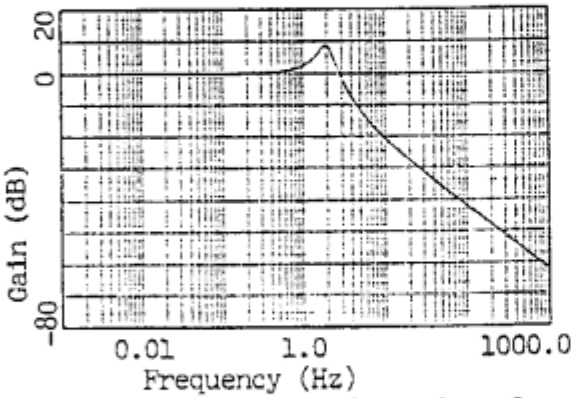

Fig. 2 Gain diagram of passive elements

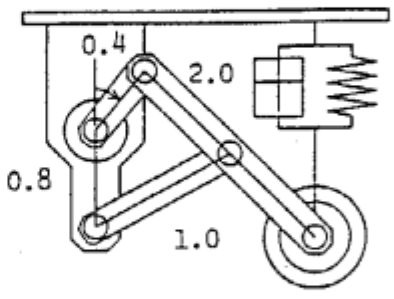

Fig. 3 An implementation of AS

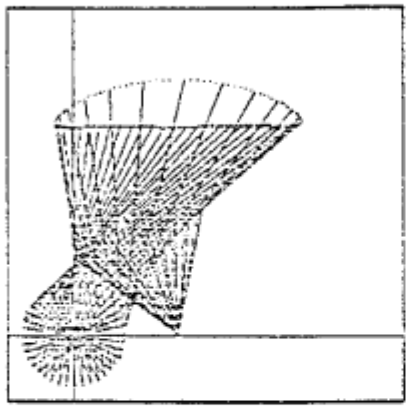

Fig. 5 Pseudo-straight line motion

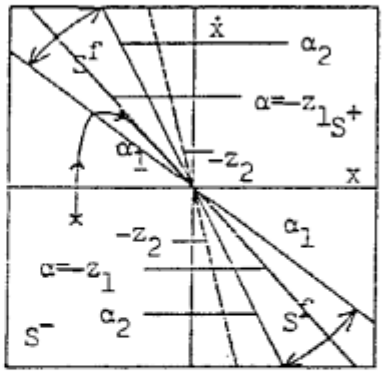

Fig. 7 A division of phase plain

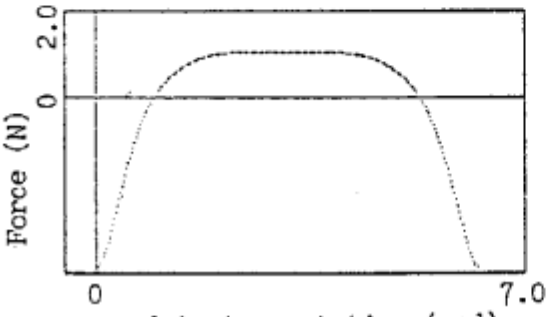

Fig. 6 Force applying at the axle

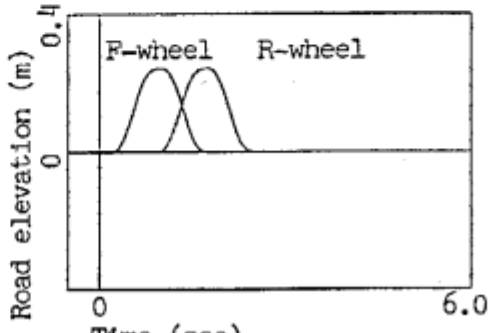

Fig. 8 Road elevation

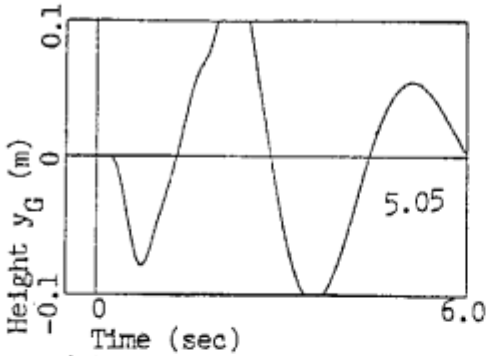

(a) Passive suspension

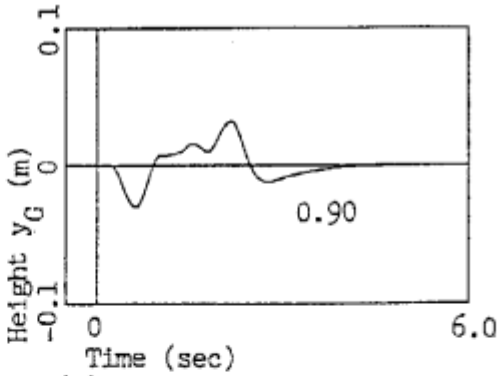

(b) Optimum regulator

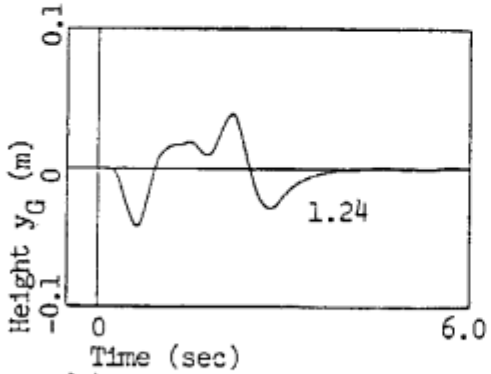

(c) Sliding mode control

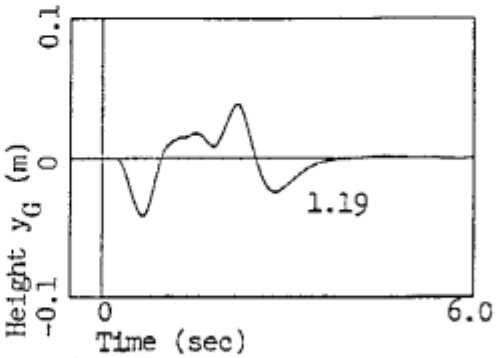

(d) Hybrid control

Fig. 9 Body height

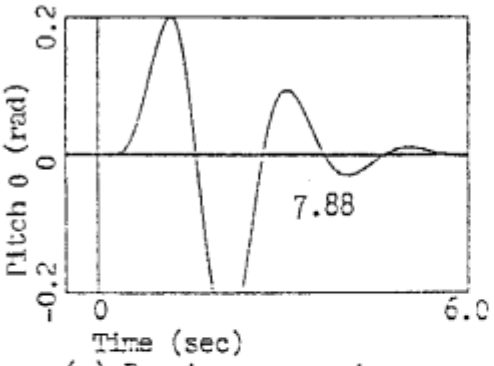

(a) Passive suspension

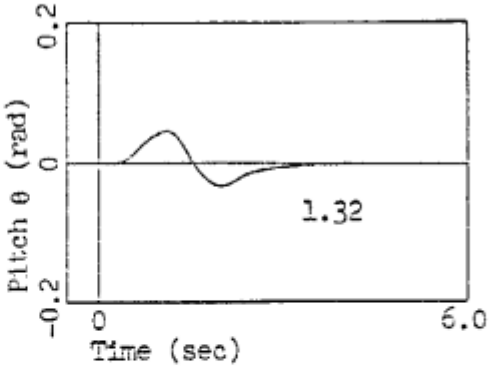

(b) Optimum regulator

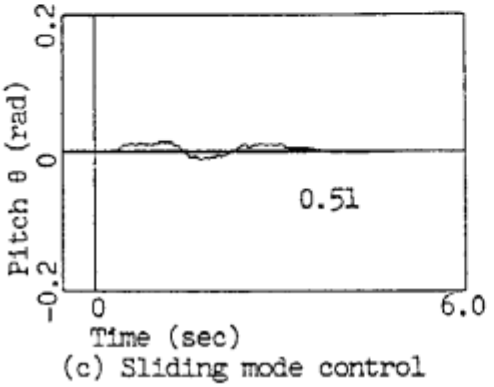

(c) Sliding mode control

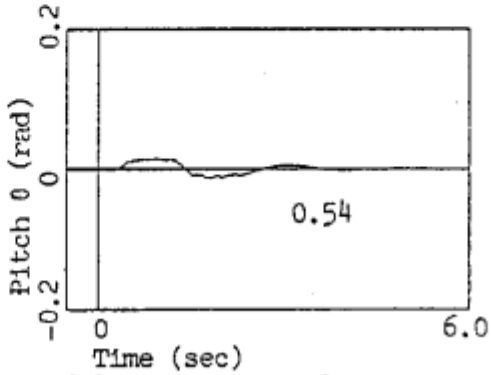

(d) Hybrid control

Fig. 10 Body tilt

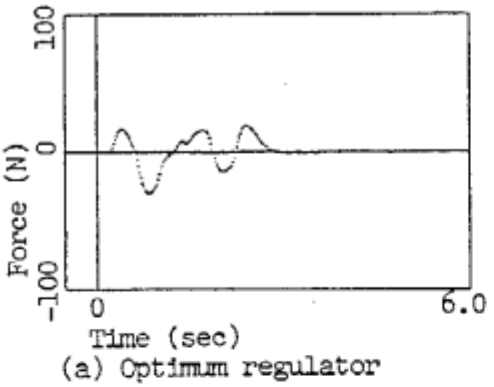

(a) Optimum regulator

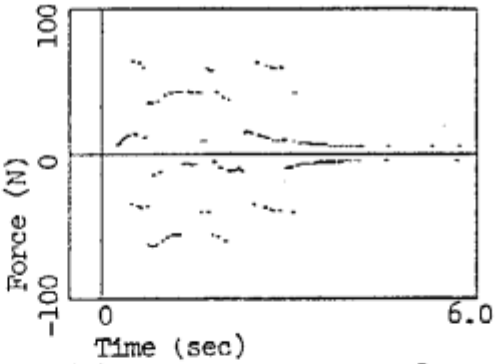

(b) Sliding mode control

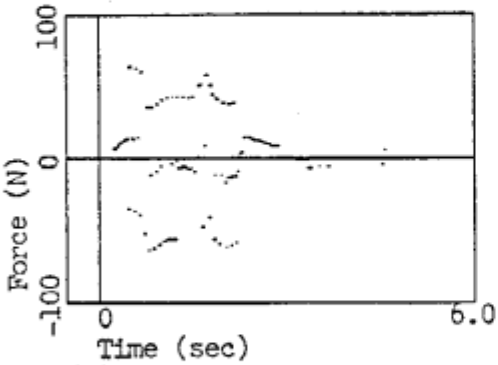

(c) Hybrid control

Fig. 11 F-wheel actuator force

Table 1 Simulation parameters

M	(kg)	50.0	$\alpha_{Y2}, \alpha_{\theta 2}$	4.0
I	(kgm^2)	10.0	$k_{\theta 1}$	100.0
L	(m)	0.75	$k_{\theta 2}$	205.0
K	(N/m)	980	k_{Y1}	100.0
C	(Ns/m)	196	k_{Y2}	103.3
$\lvert d_Y \rvert_{max}$	(N)	10.0	$Q_{\theta 1}$	1.0×10^5
$\lvert d_\theta \rvert_{max}$	(N)	5.0	$Q_{\theta 2}$	5.0×10^4
α_Y, α_θ		2.5	Q_{Y1}	2.0×10^5
$\alpha_{Y1}, \alpha_{\theta 1}$		1.0	Q_{Y2}	1.0×10^5